IEEE Access
Multidisciplinary | Rapid Review | Open Access Journal

Received May 9, 2022, accepted May 31, 2022, date of publication June 6, 2022, date of current version June 9, 2022.

Digital Object Identifier 10.1109/ACCESS.2022.3180342

Broadband, High Efficiency OMT in E-Band

GREGORY PETER LE SAGE, (Member, IEEE), AND CHRISTOPHER D. NANTISTA
SLAC National Accelerator Laboratory, Menlo Park, CA 94025, USA

Corresponding author: Gregory Peter Le Sage (lesage@slac.stanford.edu)

This work was supported in part by the U.S. Government.

ABSTRACT A high-performance, broadband E-Band orthomode transducer (OMT) was designed and fabricated for a dedicated frequency converter. Cross-polarized signals between 71 and 86 GHz, received in a TE_{11} mode circular waveguide needed to be split into separate horizontal and vertical polarization channels. The purpose of the OMT is to service the 71−76 and 81−86 GHz licensed communication bands. The main goal of OMT design is maximized transmission across the design bandwidth. Every fraction of a dB lost before the first low noise amplifier is a direct loss in SNR for the overall system. Several different design approaches were simulated, and several OMT's and ancillary components were built and tested. In the end, practical limitations determined the final path of the completed device. The final product performed several tenths of a dB better than commercially available devices and better than most reported in academic literature. Lessons learned included which construction techniques worked and did not work, as well as what compromises are acceptable.

INDEX TERMS Orthomode transducer, E-Band, microwave, polarization, bandwidth, efficiency, insertion loss.

I. INTRODUCTION

An OMT is also known as a polarization duplexer [1]. It is used to combine or separate two orthogonally polarized microwave signal paths. This may divide a satellite uplink and downlink path on the same antenna or increase signal bandwidth with separate information carried in the two orthogonal channels on the same antenna. Common uses for OTM's are VSAT terminals and terrestrial microwave communication channels. As worldwide communication increases in bandwidth, e.g. 5G, frequencies naturally increase. Since antenna gain for a parabolic reflector scales as $1/\lambda^2$, smaller antennas can carry larger bandwidth and more information can be communicated. Use of orthogonal E-Band RF streams is a natural progression for terrestrial communication.

There are three basic approaches to OMT's. Opposite the common port, type 1 includes a main arm and a side arm (e.g. [2]–[4]). Type 2 uses a main arm and a pair of symmetrical side arms (e.g. [5]–[7]). Combining the outputs of symmetrical side arms is required for a complete OMT. Type 3 uses a symmetrical pair of ports for both the main and side arms (i.e., for both polarizations) (e.g. [8]–[13]). Type 1 is a direct transition from square to rectangular waveguide with an orthogonal side arm. Reactive components are required to match the side arm. Good isolation and low return loss are difficult to achieve over a broad bandwidth using this approach. With type 2, the side arm is split into symmetrical ports. Isolation over a broad bandwidth is possible. Bøifot [5] is type 2 with reactive matching pins and a septum. With type 3, both arms are split into two symmetrical ports. The splitting junction forms a turnstile. For the cases with split output ports, these must be combined into single channels, making type 3 inherently more complex. The E-Band project ultimately used a type 3 turnstile OMT and microstrip combining of four waveguide output ports.

The design process involved simulating multiple variations of an OMT, often duplicating and scaling what could be found in academic literature. Mechanical limitations were quickly encountered. Very complex designs were not compatible with conventional CNC machining since object details were obscured. Any feature that cannot be accessed from a single direction, e.g. a channel that turns or widens away from the cutting direction, cannot be machined. An unsuccessful attempt was made to use additive manufacturing. A method that proved surprisingly successful was using very flat plates pressed together to build complex devices. The OMT presented is used only for received signals, so high RF power is never encountered. Pressed together flat plates

The associate editor coordinating the review of this manuscript and approving it for publication was Bhaskar Prasad Rimal.

in high RF current regions are incompatible with high power operation because arcing would occur. Since all WR10 and WR12 flanges operate by pressing together flat plates, it is not surprising that flat plates work, but the broad walls of waveguide sections were also split in this way. Very good machining tolerance, down to ± 0.2 mils (5.08 μm) was found to be required for best performance.

The new result that has been demonstrated is that a conventionally CNC machined OMT operated over 71−86 GHz can demonstrate a measured insertion loss of 0.1−0.2 dB. This is almost a full dB better than commercial equipment, and several tenths of a dB better than most reported results in academic literature in this frequency range. As an example, the Sage Millimeter SAT-FE-12212-S1 has a typical insertion loss for the horizontal port of 1.2 dB and the vertical port of 0.8 dB with waveguide output [14].

II. DESIGN ALTERNATIVES INVESTIGATION

One of the first OMT designs simulated was a turnstile (circular waveguide input with four orthogonal rectangular waveguide outputs) with a simple matching element (a cylinder, dome, pyramid and cone were tried) in the base of the junction. Each of the four ports give half of the H or V output signals. Fig. 1 shows such a design. The circular input waveguide has a radius of 1.59 mm. The rectangular waveguides are WR12. The cylindrical bump has radius 1 mm and optimized height 0.33 mm. This is an HFSS vacuum model, so the walls are PEC. Simulation with HFSS [15] showed 3.2 dB of insertion loss, per port, at 71 GHz and 3.7 dB at 86 GHz. Assuming efficient signal combining, this represented an OMT design with better than 0.7 dB of insertion loss. Similar devices have been described going back many years [16], [8], [17].

A type 1 OMT was devised in simulation by using a side port, a septum, and a matching aperture. The type 1 OMT is very commonly applied to terrestrial communication systems due to its simplicity and low cost [2]. This design, shown in Fig. 2, used WR12 waveguides with a square input port of dimensions 3.0988 mm. The side coupling aperture is 2.0988×0.5494 mm. This is an HFSS vacuum model, so the walls are PEC. The insertion loss was a fraction of a dB at 71 GHz but grew to 6 dB at 86 GHz. As reported in literature, bandwidth of this device is limited.

A septum OMT based on the design presented in reference [18] (see also [19]) was scaled to E Band, as shown in Fig. 3, and simulated in HFSS. The input is square waveguide 3.0988 mm on a side. The tallest part of the septum is 3.0988 mm, and the shortest is 0.4682 mm. Septum width was 0.25 mm. Individual septum widths and heights were optimized for minimum insertion loss. This is an HFSS vacuum model, so the walls are PEC. Insertion loss was approximately 1 dB, but isolation achieved (H signal in V port and V signal in H port) was only 6 to 8 dB. This can be considered a type 1 with no real distinction between main and side arms.

An entirely different approach was found in another conference paper [20] which involved four microstrip antennae in a shorted circular waveguide. Applying the HFSS optimizer in this approach, a coupling of the relevant polarization to each of the four ports of 3.2 dB was achieved in the design shown in Fig. 4, so insertion loss was 0.2 dB, assuming effective signal combination. This is a great result. Each of the four microstrip probes was optimized with final probe dimensions 0.65033 mm wide $\times$ 0.80156 mm long with a matching microstrip width of 0.27016 mm and length of 0.2433 mm. Microstrip input width was 0.317 mm, creating 50 Ω lines. The substrate is Rogers RO3003G2 with thickness 0.127 mm. Conductor and ground plane thickness was 0.035 mm.

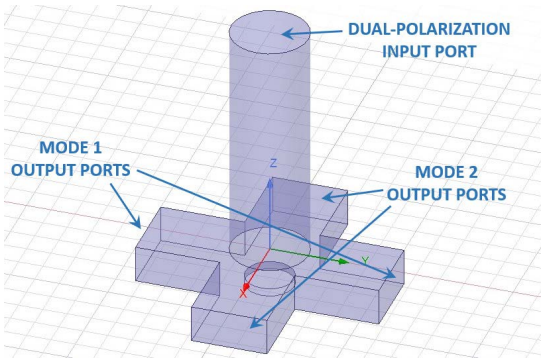

FIGURE 1. Type 3 turnstile splitter with 0.7 dB simulated insertion loss.

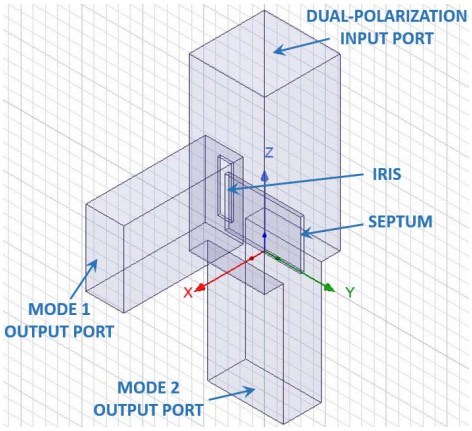

FIGURE 2. Type 1 simulated OMT.

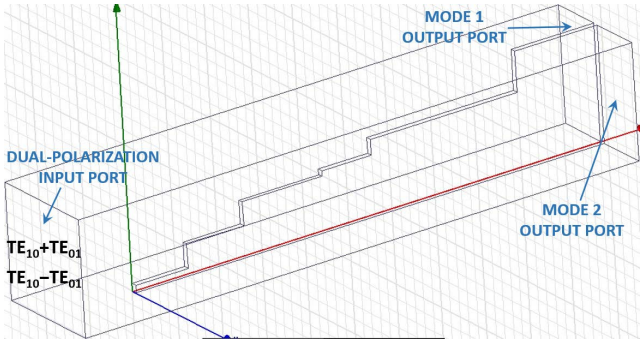

FIGURE 3. Scaled simulated septum OMT.

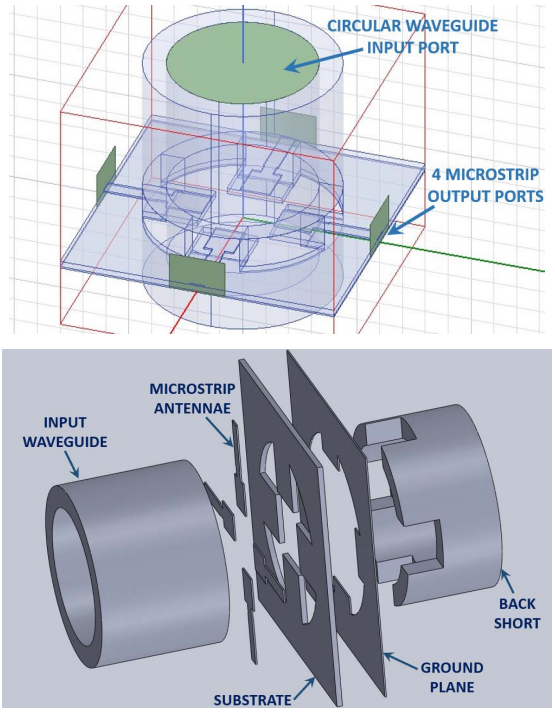

FIGURE 4. Four-port microstrip OMT: 0.2 dB simulated insertion loss.

The WC13 pipe was modeled as copper. The problem is that the pairs of outputs need to be combined, which requires the microstrip lines to cross. The referenced publication used ''crossover'' devices and ''dummy overpass'' symmetry devices to accomplish the microstrip crossing. The authors of [12] employ a similar approach in coaxial transmission line. It was decided that this complication was too difficult for the present application.

A two-sided microstrip board avoids the requirement for crossovers. For a four port microstrip OMT of this alternate configuration, a design with simulated insertion loss of 0.28 dB was achieved (see Fig. 5).

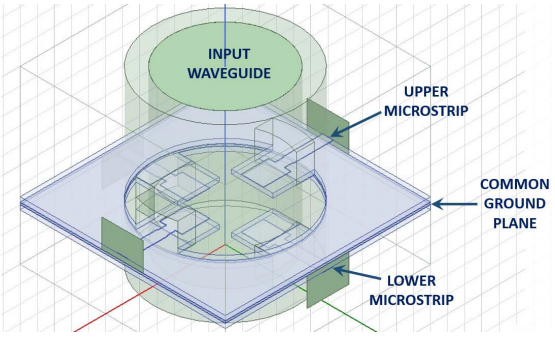

FIGURE 5. Four-port microstrip OMT with two-sided circuit board: 0.28 dB simulated insertion loss.

A microstrip output version of this design using passive 180° combiners achieved insertion loss better than 1.5 dB. In final estimation, it was decided that the circuitry would be too complex with a two-sided board.

An article that emphasized the use of additive manufacturing to produce dual polarized slot antennae [3] included a type 1 OMT. The design was scaled to E-Band and simulated in HFSS. The 3D model, shown in Fig. 6, was created in Solidworks based on scaled dimensions shown in the publication. It was modeled with PEC. It achieved better than 0.26 dB and 0.63 dB insertion loss at 71 and 86 GHz in simulation. Isolation (V signal in H port and H signal in V port) was 55 dB. The design in the publication was modified to remove obscuring features and the device was CNC machined in aluminum. The measured insertion loss (see Fig. 7) of the CNC machined aluminum device was 1.5 dB.

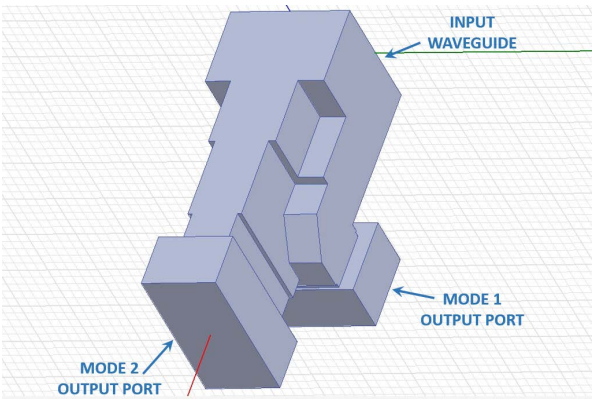

FIGURE 6. Successful type 1 OMT design: simulated insertion loss 0.26 dB.

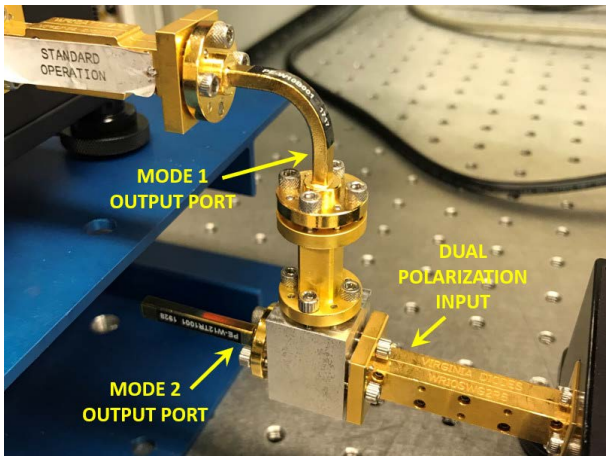

FIGURE 7. CNC machined type 1 OMT under measurement.

A type 3 turnstile OMT with waveguide combined outputs was simulated with microstrip launchers, as illustrated in Fig. 8. Insertion loss of the waveguide to microstrip launcher ranged between 0.18 and 0.48 dB between 71 and 86 GHz. The insertion loss of the OMT and launchers was between 0.2 and 0.77 dB. This HFSS model used PEC. The circular input had crossed polarization ports defined, and the microstrips were the output ports. This design is based on the four-port turnstile OMT with the addition of waveguide combiners.

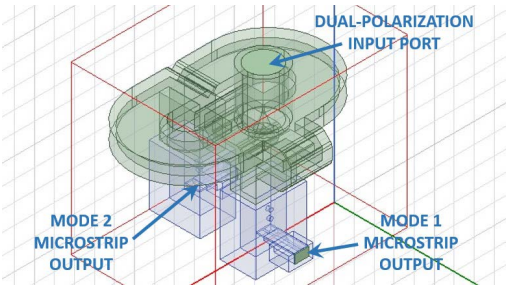

FIGURE 8. Simulated type 3 turnstile OMT with waveguide to microstrip launchers to provide microstrip outputs.

The best simulation result for a waveguide to microstrip launcher was 0.172 to 0.177 dB between 71 and 86 GHz. This is the design that was ultimately used in the final built device. Optimization included multiple widths of microstrip, changes in probe depth, and changes to the distance from the back wall of the shorted waveguide.

This launcher design used no matching posts. It was based on the custom 2.7 mm × 1.18 mm waveguide design used for the turnstile OMT. Four smooth taper widths and lengths of microstrip were optimized by HFSS (see. Fig. 9). The full optimization process required several days using 64 processors and 500 GB of RAM. Smooth tapers were selected due to observation of measured errors with fabricated microstrip dimensions. Smooth tapers were expected to be produced more accurately. The substrate is 5 mils thick Rogers RO3003G2.

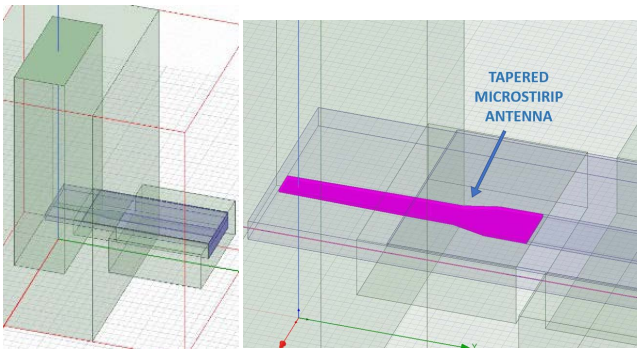

FIGURE 9. Waveguide to microstrip launcher design and detail of the tapered microstrip geometry for optimized impedance match.

The type 1 OMT that had been CNC machined with 1.5 dB of measured insertion loss was 3D printed using SLA and was electroplated with copper, as seen in Fig. 10. This device was measured and had insertion loss of 11 dB at 71 GHz. It was a failure, possibly due to the relatively low resolution of 3D printing (50 μm compared to CNC $\sim$5 μm). Given the physical access to all internal surfaces, plating was probably successful, so that was unlikely the cause of failure. The CNC machined version held measured tolerances of 0.2 mil (5.08 μm). The tolerance of SLA 3D printing is 50 microns. Simulation with HFSS varying internal parameters showed that large variation (10 or more microns) quickly degraded performance. This type of OMT cannot be effectively

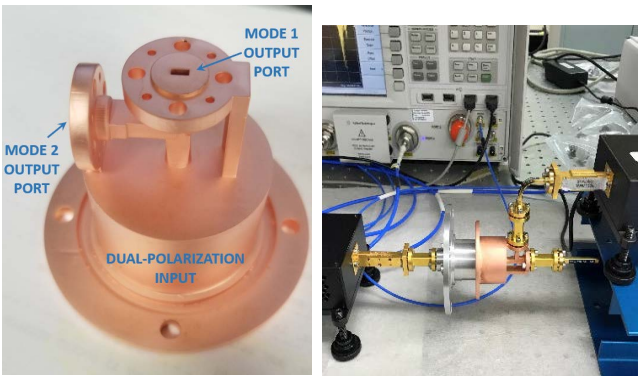

FIGURE 10. 3D printed type 1 OMT and measurement setup.

3D printed with an expectation of good performance. Other published 3D printed OMT's in this frequency range have been successful, so likely their choice in design is more forgiving of dimensional errors.

Successful OMT designs using 3D printing have been presented [21], though at the 7.2−8.2 GHz range, where tolerances are looser by more than a factor of 20. The C Band design presented used a split structure and electroless copper.

The device we tried printing is a type 3 turnstile OMT with matched E Plane combiners. The unit was DLP 3D printed and silver electroless plated using Tollen's reaction. Its operating frequency range was W-Band 75−110 GHz. Insertion loss of 0.5 and 0.6 dB (simulated 0.29 dB) was reported with isolation of 28 dB. This device was 3D printed. We were not able to test a 3D printed version of the turnstile OMT since we only have access to electroplating. The electrostatic process requires physical access to all surfaces that will be plated. The turnstile version with waveguide combining has many obscured surfaces on the inside that would not be successfully electroplated.

A CNC machined waveguide to microstrip launcher was separately simulated, built, and tested (see Figs. 11 and 12). This was important since the final device included waveguide to microstrip transitions and performance needed to be verified. Simulated insertion loss was 0.3 down to 0.16 dB over 71−86 GHz. The device was CNC machined and measured.

Measured insertion loss was 2−3.4 dB over the frequency range 71−86 GHz. The loss of the coaxial transition is unknown. Both the CNC machining tolerances and circuit board printing tolerances affected the measured result compared to simulation. Analysis of variation of dimensions in both the OMT body and microstrip showed that the measured performance was predictable. The CNC machining company produces a report showing all dimensional measurements compared to design. Errors were in the range of 0.4 mils in the worst cases. The microstrip was measured in-house with a laser confocal microscope. Microstrip errors were in the range of 0.5 mils.

In order to separate the effect of the waveguide to microstrip launcher, a four-waveguide output turnstile splitter was designed and built using CNC machining.

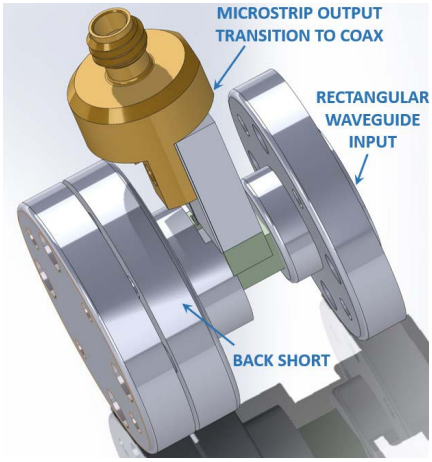

FIGURE 11. Waveguide to microstrip launcher CAD model.

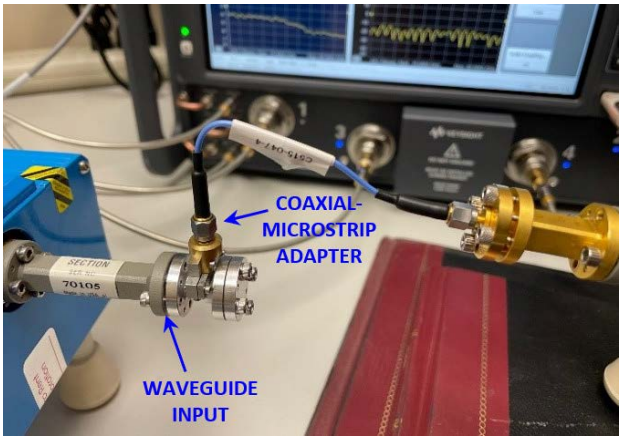

FIGURE 12. CNC machined waveguide to microstrip launcher testing.

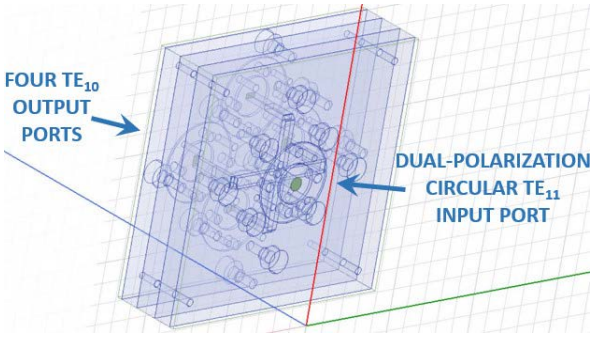

FIGURE 13. Four waveguide output turnstile OMT.

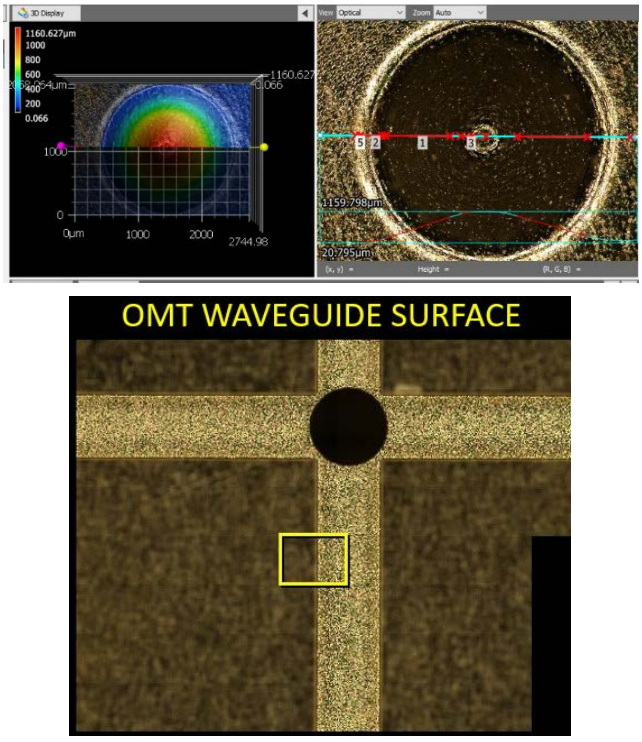

FIGURE 14. Turnstile OMT laser confocal microscope characterization of matching cone and radial waveguides.

The model is a stack of plates, illustrated in Fig. 13, that allows the body of the four-port turnstile to be machined. In a similar fashion to previous simulations, a cross polarized circular input port was used with TE_{10} waveguide outputs. Simulated insertion loss was between 0.08 and 0.115 dB over the frequency range of 71−86 GHz for a PEC model. The measured port insertion loss averaged 4 dB with suck-outs at 5 dB. That represents insertion loss between 1 and 2 dB, considering 3 dB splitting.

The four-waveguide output waveguide OMT was measured using the same laser confocal microscope used to characterize microstrip circuits. The CNC tolerances were verified. Measured surface roughness was worse than expected. Chemical gold plating causes formation of dendrites that add to surface roughness (see Fig. 14). Vapor gold plating would have been preferable. Since dimensions measured well, surface roughness was likely to blame for the difference between simulated and measured results.

One key concern about using flat plates pressed together to build the OMT was whether splitting a waveguide by opening one broad wall with seams at the corners would work. The strongly preferable way to split a waveguide is to divide the broad wall in the center where currents do not cross [22]. Short waveguide runs with such a split between mitered bends were built and tested relying in turn on plate flatness alone, a knife edge and an indium gasket seal for RF contact.

The test structure model for the waveguide with the broad wall split is shown in Fig. 15. The purpose of this test structure is to show the loss incurred by splitting the edges of a waveguide broad wall at E Band. Simulation with HFSS only shows the loss of the waveguide length since simulation sees the joints as perfect.

Shown in Fig. 16 are a fabricated version and its test setup. Simulated insertion loss for this device was 0.2 dB, due only to waveguide loss. The indium gasket model had

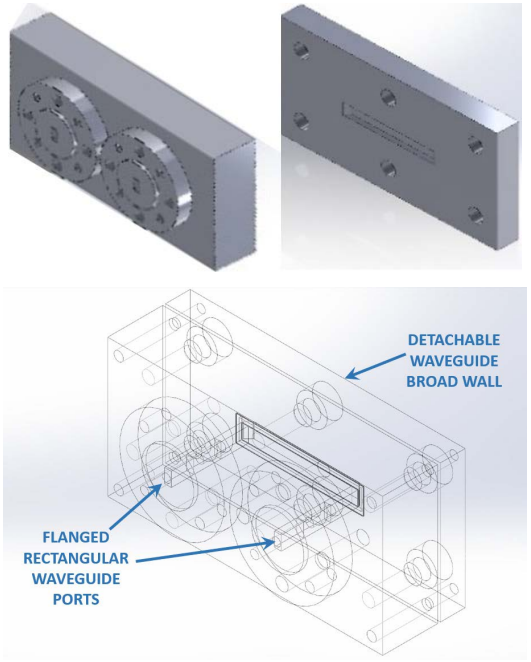

FIGURE 15. Pressed broad wall opening waveguide test fixture.

insertion loss of 0.55 dB. The knife edge model had insertion loss of 0.65 dB. The flat plate model had insertion loss of 0.85 dB. These three units performed as expected. The indium seal is best, followed by the knife edge. The indium sealed waveguide added less than 0.35 dB of loss, assuming a measured waveguide would have had slightly higher loss than the simulated result.

A CNC-machined turnstile splitter interfaced via microstrip transitions to circuit board with coaxial output connectors was fabricated. Fig. 17 shows the model. This tested the turnstile OMT with microstrip transitions, which models the final built device without amplifiers installed. The simulated coupling of this OMT up to each coupled microstrip output was between 3.5 and 3.63 dB between 71 and 86 GHz, corresponding to insertion loss between 0.49 and 0.62 dB.

The measured device (see Fig. 18) had an insertion loss of 1 dB (coupling of 4 dB) between 71 and 86 GHz, with suck outs down to 3 dB (coupling of 6 dB). The microstrip to coaxial transitions are uncalibrated, so their contribution to loss is unknown. This was another measurement intended to prove that a device could be fabricated with reasonable insertion loss as it is the front end of a receiver. Any loss in this component, before the first amplifier directly degrades the signal to noise ratio of the receiver. Measured loss of 1 dB, especially with unknown coaxial transition loss was considered to be reasonable.

III. TURNSTILE DESIGN

In launching or extracting power between rectangular waveguide and a particular mode in circular waveguide, an obvious approach is to couple radially, exploiting field symmetry and an end short, as is done in the TM_{01} launcher [23] and the

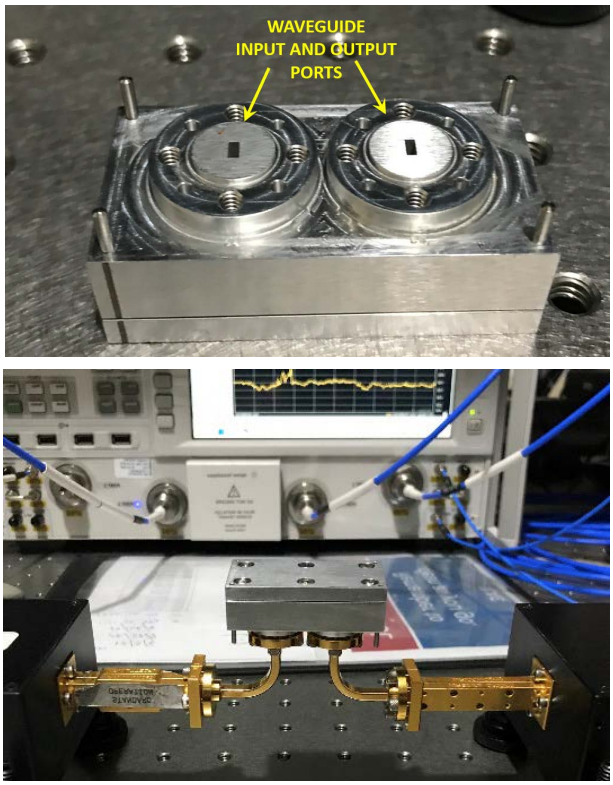

FIGURE 16. Waveguide broad wall opening test fixture measurement.

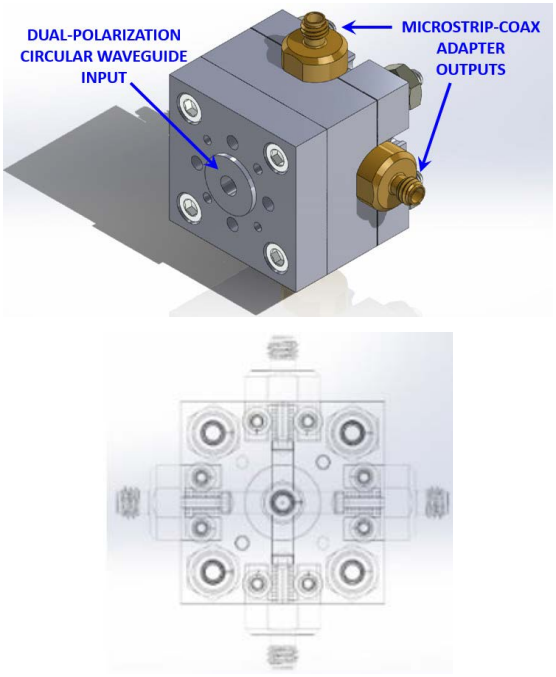

FIGURE 17. Coaxial output waveguide-to-microstrip OMT, CAD image and transparent end view.

TE_{01} four-way splitter [24]. For the TE_{11} mode of our antenna waveguide, four radiating rectangular waveguides with their broad walls in the perpendicular shorting plane provide the

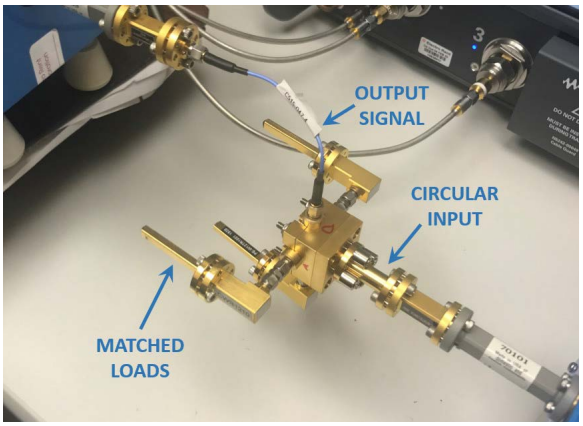

FIGURE 18. Coaxial output microstrip OMT measurement.

desired coupling. Each pair of opposite waveguides couples to one and only one of the perpendicular polarizations.

Such a "turnstile" design for separating polarizations has been frequently employed. A centered matching element on the short can suffice to achieve good and surprisingly broadband transmission. We tried a dome and a cylindrical button and found best results using a blunt cone to turn the fields, varying its lower and upper radii and height for optimal match. Our circular waveguide is WC13 (3.175 mm diameter). In addition to TE_{11}, this supports the TM_{01} mode above 72.3 GHz, but reflection into it is ruled out by the symmetry of the geometry, so it does not enter into the matching problem. With no requirement to interface to a standard waveguide, rectangular dimensions of 2.7 mm × 1.18 mm were chosen, set roughly midway between cutoff at our low frequency and overmoding at our high frequency and using a low height to help the impedance match. Fig. 19 shows the resulting turnstile junction (1/4 geometry) and a return loss plot below −31 dB across the 71−86 GHz range.

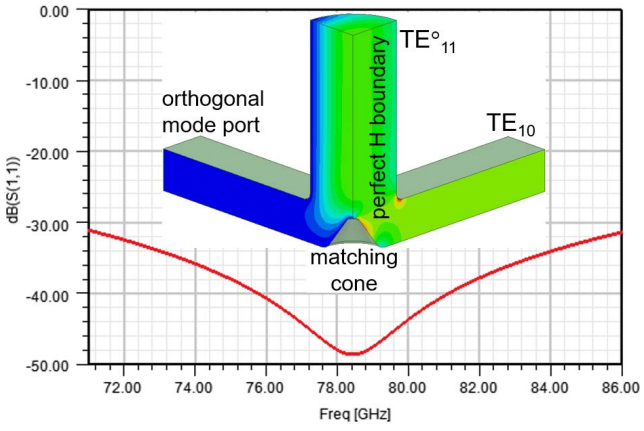

FIGURE 19. Quarter-view of the four-output turnstile design geometry, with E-fields, over a plot of S_{11} match across design bandwidth.

To complete an OMT with such a turnstile, the signals from each pair of ports must be combined to yield two outputs. This was initially accomplished in an all-waveguide design, but fabricability concerns led us to pursue combining after transition to microstrip. With optimized E-plane bends added to bring the ports to the board as shown in Fig. 20a, return loss was essentially unaffected, and the simulated insertion loss with copper conductivity was 0.034−0.044 dB (∼0.9%).

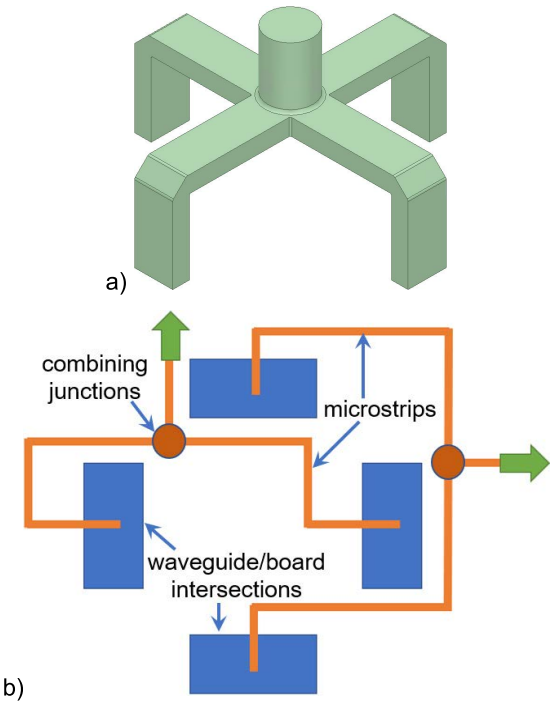

FIGURE 20. a) Full turnstile with bends toward board and b) schematic illustrating use of inner and outer broad wall microstrip transitions to enable combining without the need for crossovers.

The breakthrough for the four-output turnstile approach was the realization that with the four waveguides interfaced with the microstrip circuit board through E-plane bends at sufficient spacing, the microstrip transitions can be brought out from the inner or outer broad walls. This allows opposite channels to be combined on the board as shown in Fig. 20b, with one line passing between the other port pair, thus completing the OMT without the need for microstrip crossovers or a two-sided board. The common phase of each transition pair also allows their combining with equal path lengths for maximal match bandwidth. This turnstile waveguide/microstrip OMT configuration was selected as the final version for the project.

IV. FULL WAVEGUIDE TURNSTILE-BASED OMT

When it was realized that the stacked plate CNC construction applied to the board-combined turnstile might be applied to it as well, the waveguide-combined turnstile OMT was revisited. The combining is accomplished by bringing two ports together through E-plan mitered U-bends to combine through an E-plane T and bringing the other pair together through H-plane swept U-bends to also combine through

an E-plane T. To facilitate flanging and testing, the output dimensions were adjusted to those of WR12 (3.0988 mm × 1.5494 mm). The pre-combined waveguide was made half-height to retain the low-height benefit at the turnstile junction and to simplify the T junctions, now essentially conjoined mitered E-plane bends. The matching cone was re-optimized, and all bends matched at our center 78.5 GHz frequency.

The resulting compact design has both output ports pointing in the same direction, facilitating interfacing with a circuit board, unlike the similar but more complex since-published "Swan Neck" design [9]. It is also simpler and more compact and symmetric than the similar Ku band designs recently presented in [10]. The full geometry and functionality are illustrated in Fig. 21. Despite the H-plane bends breaking symmetry, simulated discrimination remains better than 70 dB. The return loss is between 21 and 34 dB across the 71−86 GHz range, and the insertion loss with copper conductivity between 0.045 and 0.117 dB, with the H-plane path ∼0.036 dB more lossy than the shorter E-plane path. Surface roughness can be expected to increase realizable insertion loss, but waveguide combining should be considerably more efficient than microstrip combining.

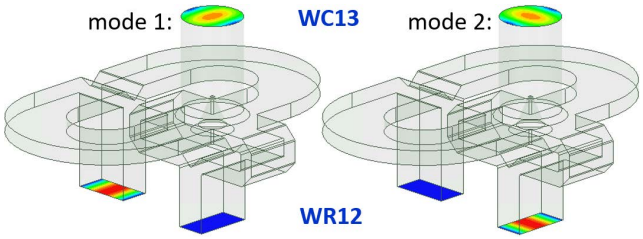

FIGURE 21. Broadband turnstile-based full waveguide OMT with polarization selection.

The delivered OMT has four waveguide outputs that are combined electronically in microstrip, but it is possible to design a two-waveguide output OMT that can be successfully machined. Fig. 22a illustrates a model of stacked plate construction, while Fig. 22b shows a design modification made to accommodate flange connection in the test model.

There are three blocks involved in the construction. The complex shapes of the E-plane combiners are embedded in machined waveguide sections. The conical structure of the turnstile junction is part of the middle block. The separate parts in stacking order are shown in Fig. 23. This is the innovation that enabled this structure to be CNC machined. From any direction, CNC machining can only cut in one direction. No obscured features can be machined. An obscured feature is simply any feature that is not visible from the direction of machining. Examining the vacuum model in Fig. 22b, there are obscured features looking from any direction. This structure cannot be made using CNC machining as a single monolithic unit.

The method of drawing this object for fabrication involved subtraction of the vacuum OMT from a single block and splitting the block in to three sections. Once it was verified

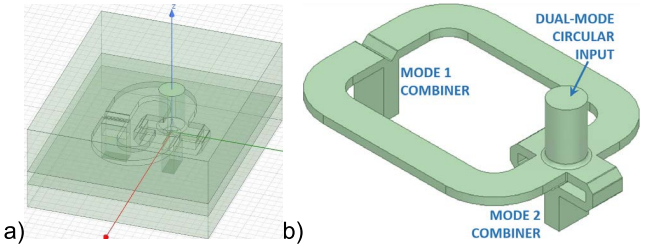

FIGURE 22. a) Stacked-contruction full waveguide OMT and b) extended version spaced for flange connection (vacuum model).

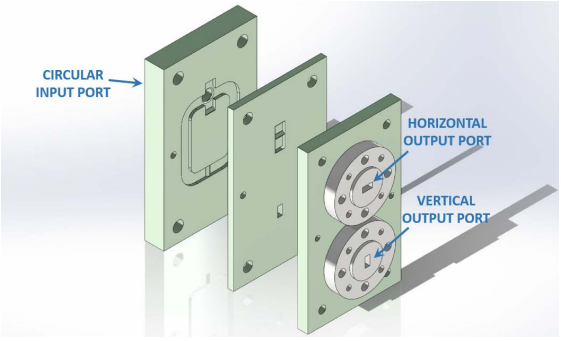

FIGURE 23. Stacked, combined output OMT.

with a CNC shop that all three parts could in fact be made, they were machined, assembled (as illustrated in Fig. 24) and tested. The innovation of this design is that the obscured features that prevent CNC machining of the complete device are exposed by the structural splits so that each piece can be successfully machined.

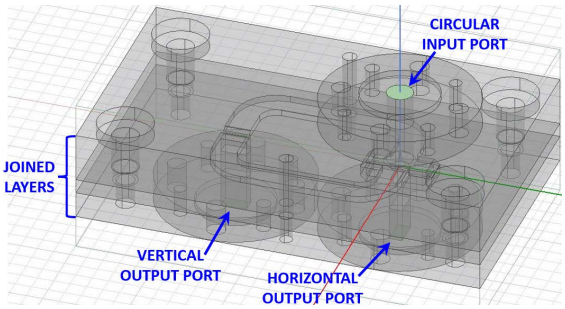

FIGURE 24. Combined output OMT HFSS model.

This OMT has two waveguide outputs. The simulated insertion loss between 71 and 86 GHz is between 0.1 dB for horizontal polarization and 0.2 dB for vertical polarization with waveguide output. The second arm was extended to accommodate two WR12 flanges. Vertical polarization has the longer path length of waveguide in the device, leading to slightly higher loss. The device was CNC machined with copper, and indium seals were used to make RF contact between the three plates (see Fig. 25). Splitting the structure has the disadvantage of relying on joined pieces to build the OMT. Use of indium seals was shown in the waveguide tester to provide the best performance.

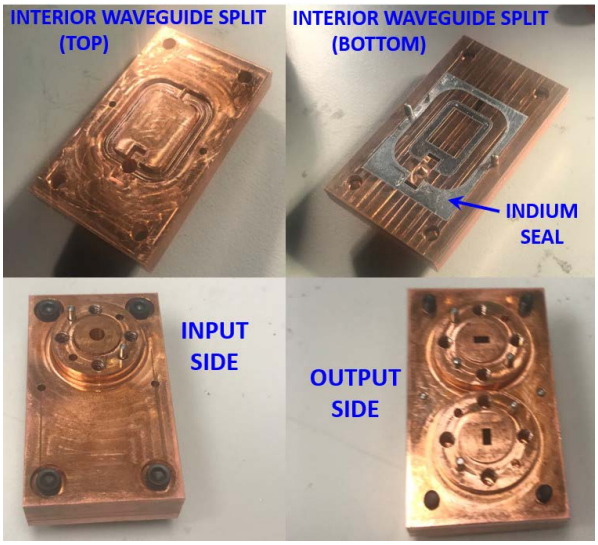

FIGURE 25. Two waveguide output stacked OMT fabricated part views.

The combined output E-band OMT, assembled and tested (Fig. 26), was found to function between 60 and 95 GHz, though it was designed for operation between 71 and 86 GHz. Simulated and measured insertion loss for vertical and horizontal polarizations to their respective combining ports are shown in Fig. 27.

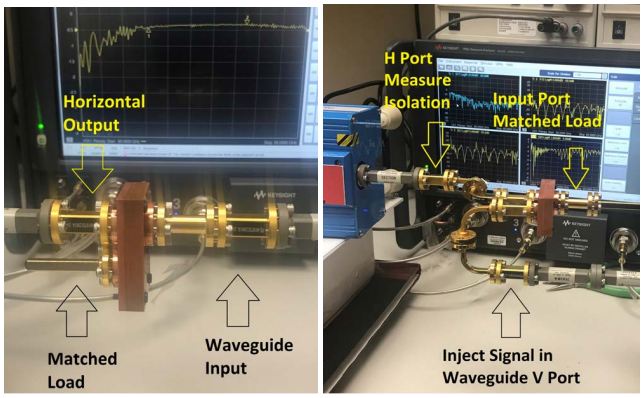

FIGURE 26. Two waveguide output stacked OMT measurement of insertion loss and isolation.

The circular waveguide cutoff frequency is 55.34 GHz, which explains the low frequency cutoff. The rectangular waveguide, WR12 becomes overmoded (TE_{20}) at 96.74 GHz, which explains the failure at the upper limit.

The measured insertion loss was very close to simulated values. This is an important result, because it demonstrates that split structure fabrication with indium seals does not noticeably degrade performance from the best one can expect. At roughly 0.1−0.15 dB for one polarization and 0.2−0.3 dB for the other (due to extra path length for flanging), our results compare favorably to those published elsewhere for OMTs in this frequency band. For example, Wollack [25] reports <0.2 dB, Chen [19] ∼0.2–0.3 dB, Navarrini [6] ∼0.1−0.3 dB

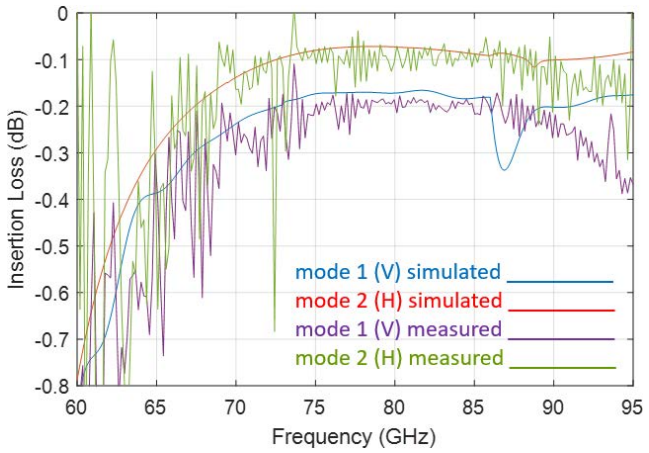

FIGURE 27. Combined output OMT vertical and horizontal insertion loss.

and Chung [26] ∼0.25−0.45 dB. Typical insertion losses of commercially available OMTs are significantly worse, on the order of 0.8 dB (e.g. [14], [27], [28]).

The measured values of S_{11} and S_{22} were better than −10 dB between 60 and 95 GHz. Isolation between the vertical and horizontal outputs was approximately 45 dB.

V. CONCLUSION

The goal of this effort was production of a low insertion loss OMT for the 71-76 and 81-86 GHz bands. After many separate efforts with varying degrees of success, a reliable four port waveguide output device and a higher performance two waveguide output port device were designed, built, and tested. Valuable lessons were learned in the process of producing the final designs. Some negative conclusions are included here.

Chemical gold plating of aluminum parts resulted in surprisingly rough surfaces. Chemical plating of aluminum creates "dendrites" on the surface. Vapor gold deposition is preferable to achieve flat surfaces. The CNC machining company who built all the parts for this experiment said that they could achieve flatter surfaces through careful machining than through lapping. One disadvantage of vapor plating is that it is line of sight only. The inside of waveguides could not be vapor plated. Switching to use of copper improved conductivity and performance.

Electroplating cannot work for the OMT parts since electrostatic fields cannot penetrate past waveguide bends. That precluded 3D printing of the waveguide combined turnstile OMT.

Aluminum soldering has about half the electrical conductivity of bulk aluminum. It is structurally useful but not electrically advantageous.

Microstrip tolerances did not hold well. They were off by mils in some cases. Simulation showed fractions of a dB degradation in insertion loss due to the microstrip errors.

Switching to positive lessons, a laser confocal microscope is good for measuring dimensions and surface roughness

for metal and circuit board parts. It was used to characterize both the machined OMT and microstrip circuits. The CNC machining company provided measurements of all part dimensions using a laser confocal microscope to compare specified tolerances. In one case, a 2 mil error was found, but simulation showed that it had small impact on device performance.

For the final OMT, copper was used, and the CNC machine shop held best possible surface finish for mating surfaces.

A requirement for an E-Band OMT resulted in extensive investigation: simulation and measurement of many options. Varying degrees of success and failure led finally to a design with insertion loss about as low as achieved in this frequency range ($\sim$0.1$-$0.2 dB) and a very wide fractional bandwidth of operation ($\sim$40%, with an application goal of 20%).

ACKNOWLEDGMENT

The authors would like to acknowledge the important contributions of Daniel D. Van Winkle, a SLAC Engineer in the development of the E-Band OMT. He performed many important RF measurements and gave advice about design considerations that led to ultimate success.

REFERENCES

[1] [Online]. Available: https://en.wikipedia.org/wiki/Orthomode_transducer
[2] G. Rahul, "Design and fabrication of compact and high performance C band OMT," *Int. J. Microw. Eng. (JMICRO)*, vol. 4, nos. 3–4, Oct. 2019.
[3] M. Garcia-Vigueras, "Cost-effective dual-polarised leaky-wave antennas enabled by three-dimensional printing," *IET Microw., Antenna Propag.*, vol. 11, no. 14, pp. 1985–1991, 2017.
[4] A. E. Kamili, "Design and simulation of a multiband orthomodetransducer in K/Ka band for satellite communications," in *Proc. Int. Conf. Adv. Technol. Signal Image Process. (ATSIP)*, Fez, Morocco, May 2017, pp. 1–4.
[5] A. M. Bøifot, E. Lier, and T. Schaug-Pettersen, "Simple and broadband orthomode transducer," *IEE Proc. H (Microw., Antennas Propag.)*, vol. 137, no. 6, pp. 396–400, 1990.
[6] A. Navarrini and R. Nesti, "Symmetric reverse-coupling waveguide orthomode transducer for the 3-mm band," *IEEE Trans. Microw. Theory Techn.*, vol. 57, no. 1, pp. 80–88, Jan. 2009.
[7] T.-L. Zhang, "Design of broadband orthomode transducer based on double ridged waveguide," in *Proc. Int. Conf. Microw. Millim. Wave Technol.*, May 2010, pp. 765–768.
[8] A. Navarrini and R. L. Plambeck, "A turnstile junction waveguide orthomode transducer," *IEEE Trans. Microw. Theory Techn.*, vol. 54, no. 1, pp. 272–277, Jan. 2006.
[9] J. Shen and S. David Ricketts, "Compact W-band 'swan neck' turnstile junction orthomode transducer implemented by 3-D printing," *IEEE Trans. Microw. Theory Techn.*, vol. 68, no. 8, pp. 3408–3417, Aug. 2020.
[10] R. Nesti, E. Orsi, G. Pelosi, and S. Selleri, "Design of two Ku-band orthomode transducers for radio astronomy applications," *Prog. Electromagn. Res.*, vol. 163, pp. 79–87, 2018.
[11] E. Zhang, P. Zhang, and J. Qiu, "Design of a multi-band orthomode transducer for radiometers," in *Proc. Int. Symp. Antennas Propag. (ISAP)*, Phuket, Thailand, Oct. 2017, pp. 1–2.
[12] G. Engargiola and A. Navarrini, "Orthomode transducer with waveguide ports and balanced coaxial probes," in *Proc. 16th Int. Symp. Space Terahertz Technol.*, Goteborg, Sweden, May 2005, pp. 334–337.
[13] A. Tribak, "X/Ku octave-bandwidth waveguide orthomode transducer," in *Proc. TELECOM 8th JFMMA*, Marrakech, Marocco, Mar. 2013.
[14] [Online]. Available: https://sftp.eravant.com/content/datasheets/SAT-FE-12212-S1.pdf
[15] *Ansys HFSS (High Frequency Simulation Software)*, ANSYS, Canonsburg, PA, USA.
[16] M. A. Meyer and H. B. Goldberg, "Applications of the turnstile junction," *IRE Trans. Microw. Theory Techn.*, vol. 3, no. 6, pp. 40–45, Dec. 1955.
[17] Y. Aramaki, N. Yoneda, M. Miyazaki, and T. Horie, "Ultra-thin broadband OMT with turnstile junction," in *IEEE MTT-S Int. Microw. Symp. Dig.*, vol. 1, Jun. 2003, p. 4750.
[18] P. Sarasa, M. Diaz-Martin, and J. C. Angevain, "New compact OMT based on a septum solution," in *Proc. 5th Eur. Conf. Antennas Propag. (EUCAP)*, Apr. 2011, pp. 1181–1185.
[19] Y.-L. Chen, T. Chiueh, and H. F. Teng, "A 77–118 GHz resonance-free septum polarizer," *Astrophys. J. Suppl.*, vol. 211, no. 1, p. 11, Mar. 2014.
[20] G. Valente, A. Navarrini, F. Schaefer, P. Serres, and F. Thome, "Architecture of highly integrated cryogenic active planar orthomode transducer for the 3-mm band," in *Proc. 2nd URSI Atlantic Radio Sci. Meeting (AT-RASC)*, May 2018, pp. 1–4.
[21] H. Saeidi-Manesh and S. Saeedi, "Design and fabrication of orthogonal-mode transducer using 3-D printing technology," *IEEE Antennas Wireless Propag. Lett.*, vol. 17, no. 11, pp. 2013–2016, Nov. 2018.
[22] G. P. Le Sage, "3D printed waveguide slot array antennas," *IEEE Access*, vol. 4, pp. 1258–1265, 2016.
[23] C. D. Nantista and V. A. Dolgashev, "Novel accelerator structure couplers," presented at the Part. Accel. Conf., Portland, OR, USA, 2003.
[24] C. D. Nantista, "Overmoded waveguide components for high-power RF," in *Proc. 6th Workshop High Energy Density High Power (RF)*, Jun. 2003.
[25] E. J. Wollack, W. Grammer, and J. Kingsley, "The boifot orthomode junction," Nat. Radio Astron. Observatory, Charlottesville, VA, USA, Tech. Rep. ALMA Memo #425, May 2002.
[26] M.-H. Chung, D.-H. Je, and S.-R. Kim, "A broadband W-band orthomode transducer for KVN polarization observations," *J. Astron. Space Sci.*, vol. 30, no. 4, pp. 345–353, Dec. 2013.
[27] [Online]. Available: https://quinstar.com/wp-content/uploads/2012/11/QOT.pdf
[28] [Online]. Available: https://www.everythingrf.com/product-datasheet/868-1385-qmc-omt12-7815

GREGORY PETER LE SAGE (Member, IEEE) received the B.S., M.S., and Ph.D. degrees in electrical engineering from UCLA, in 1991, 1994, and 1997, respectively, all in electromagnetics.

In 2004, he was at the Lawrence Livermore National Laboratory. In 2020, he was also at the United States Government, Washington, D.C., USA. He is currently with the SLAC National Accelerator Laboratory, Stanford University. He is also a SLAC Program Developer/Manager with the RF Accelerator Research Division, Technology Innovation Directorate. He has authored and coauthored numerous journal articles and conference papers. His research interests include particle accelerators, high power microwaves, lasers, miniature electronics, power sources, 3-D printing and scanning, CNC machining, and antenna design.

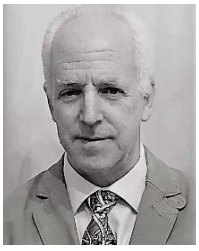

CHRISTOPHER D. NANTISTA received the B.A. degree in physics from Cornell University, in 1986, and the M.S. and Ph.D. degrees in physics from UCLA, in 1988 and 1994, respectively.

Since 1994, he has been a Staff Scientist with the SLAC National Accelerator Laboratory, he is currently with the RF Accelerator Research Division, Technology Innovation Directorate. In 2000, he was a Visiting Researcher at KEK, Tsukuba, Japan. He has authored and/or coauthored numerous journal articles and workshop and conference papers. His research interests include particle accelerators, linear colliders, high-power RF sources, RF pulse compression and distribution, beam diagnostics, and special waveguide components.